PD-Based Modulation Index Compensation for Improving the Transient Response of Three-Phase Induction Motors

1st Ihsan Auditia Akhinov*
Dept. of Electrical Engineering
Politeknik Negeri Jakarta
Depok, Indonesia
ihsan.auditia.akhinov@elektro.pnj.ac.id

2nd Rizdam Firly Muzakki
Dept of Electrical Engineering
Politeknik Negeri Jakarta
Depok, Indonesia
rizdam.firly.muzakki@elektro.pnj.ac.id

3rd Joko Slamet Saputro
Dept. of Electrical Engineering
Universitas Sebelas Maret
Surakarta, Indonesia
jssaputro89@staff.uns.ac.id

*Corresponding author: ihsan.auditia.akhinov@elektro.pnj.ac.id
Received: 2026-10-23; **Accepted:** 2026-11-02

***Abstract*— Conventional Voltage per Frequency (V/f) control with a Proportional Integral (PI) controller offers a simple approach to induction motor speed regulation. However, its transient performance can be limited during startup and load disturbances. This study proposes a Proportional Derivative (PD) based Modulation Index Compensation (MIC) strategy to improve the transient response of a three-phase induction motor drive. The proposed method operates in parallel with the PI controller, using speed error and its derivative to adjust the inverter modulation index while maintaining the conventional V/f frequency regulation structure. The method was evaluated through MATLAB/Simulink simulations using a sinusoidal pulse width modulation (SPWM) inverter with a 10 kHz carrier frequency. During startup, the PI-MIC controller reduced the settling time from 0.5090 s to 0.41965 s and overshoot from 2.0621% to 1.4497% compared with conventional PI control. Under a 5 Nm load disturbance, PI-MIC produced a slightly larger speed dip of 13.703 rpm than conventional PI control at 12.674 rpm, but achieved a lower recovery peak. The torque settling time also decreased from 0.19491 s to 0.12086 s, although the torque ripple increased. Further evaluation showed that inverter dead time affected the speed, torque, and harmonic characteristics. These results indicate that PD-based MIC improves selected transient performance indicators, while its effectiveness depends on operating and switching conditions.**

Keywords*— *Induction motor, V/f control, Modulation index compensation, Proportional derivative controller, Sinusoidal pulse width modulation.

I. INTRODUCTION

Three-phase induction motors are among the most widely used electrical machines in industrial applications because of their cost-effectiveness, high reliability, and robust operating characteristics [1]. In industrial drive systems, maintaining stable speed regulation under operating and parameter variations is essential to ensure reliable motor performance [2]. As industrial processes increasingly demand higher energy efficiency, faster dynamic response, and greater operational flexibility, improving induction motor speed control has become an important research focus in modern electric drive systems [3].

Among the available speed control techniques, scalar Voltage per Frequency (V/f) control is widely used in induction motor drives because it maintains approximately constant air-gap flux by preserving the voltage-to-frequency ratio below the rated frequency. Compared with vector control, scalar V/f control offers a simpler control structure and easier implementation, making it suitable for industrial applications that prioritize control simplicity and implementation cost [3], [4].

In practical applications, V/f control is commonly combined with a Sinusoidal Pulse Width Modulation (SPWM) based voltage source inverter to generate three-phase AC voltages with adjustable amplitude and frequency. SPWM provides high-quality output voltage through modulation index regulation while maintaining relatively low harmonic distortion, making it one of the most widely implemented modulation techniques in inverter-fed induction motor drives [5], [6].

Despite its simplicity and widespread industrial adoption, PI-based V/f control still exhibits limited transient performance under dynamic operating conditions. During startup, speed reference variations, and sudden load disturbances, the closed-loop drive may experience slower dynamic responses, resulting in longer rise time and settling time than desired. Consequently, improving the transient performance of PI-based V/f control remains an important research topic for inverter-fed induction motor drives [7], [8].

Numerous studies have sought to improve induction motor drive performance through controller parameter optimization, advanced pulse width modulation (PWM) techniques, hybrid inverter modulation strategies, and improvements in inverter output voltage quality [9]–[11]. These approaches have demonstrated significant improvements in speed regulation, harmonic suppression, voltage regulation, and overall drive performance. However, most existing studies primarily focus on controller tuning, PWM algorithm development, or inverter topology enhancement rather than adaptive voltage regulation during transient operating conditions. Consequently, the potential of utilizing the modulation index as an adaptive compensation variable to dynamically regulate the inverter output voltage and improve the transient response of PI-based V/f control remains insufficiently explored.

Motivated by this research gap, this study proposes a Modulation Index Compensation (MIC) method integrated into a PI-based V/f control system for an SPWM inverter-fed three-phase induction motor. In the proposed approach, the PI controller generates the inverter reference frequency, while a proportional-derivative (PD) controller produces an additional modulation index compensation signal based on the speed error and its rate of change. Unlike conventional

Copyright © 2026 Universitas Sebelas Maret

approaches that modify the primary V/f control structure, the proposed method enhances the inverter output voltage dynamically through adaptive modulation index compensation while preserving the simplicity of the conventional V/f strategy. The effectiveness of the proposed method is evaluated through MATLAB/Simulink simulations by comparing the conventional PI controller with the proposed PI & MIC approach in terms of rise time, settling time, overshoot, and steady-state error.

II. METHOD

A. *Proposed Control System Architecture*

Fig. 1 illustrates the proposed control system architecture for a three-phase induction motor drive based on scalar Voltage per Frequency (V/f) control using a Sinusoidal Pulse Width Modulation (SPWM) inverter. The overall control structure is based on the conventional closed-loop PI-based constant V/f control strategy [12]. In the conventional control scheme, the speed error between the reference speed (ω_{ref}), and the measured motor speed (ω) is processed by a Proportional-Integral (PI) controller to generate the inverter reference frequency. The reference frequency is subsequently converted into the corresponding voltage reference according to the constant V/f characteristic, and the resulting modulation index is used by the SPWM generator to produce the switching signals for the voltage source inverter (VSI).

To improve the transient response of the conventional V/f control system, this study introduces a Modulation Index Compensation (MIC) block based on a Proportional-Derivative (PD) controller. The proposed method generates an additional compensation signal from the speed error and its rate of change, and the compensated modulation index is then applied to the SPWM generator to regulate the inverter output voltage dynamically. This approach is consistent with the established role of modulation index in determining inverter output voltage and harmonic performance in SPWM-based inverters [12]–[14].

The proposed method extends the conventional V/f control architecture by incorporating an additional Modulation Index Compensation (MIC) path based on a Proportional-Derivative (PD) controller. Unlike the conventional V/f strategy, which regulates only the inverter frequency through the PI controller, the proposed MIC adaptively adjusts the inverter voltage amplitude by modifying the modulation index during transient operating conditions. Since the modulation index directly influences the output voltage magnitude and waveform quality of SPWM-based inverters, adaptive modulation provides an additional voltage regulation mechanism while preserving the simplicity of the conventional V/f control structure [15]–[17]. Consequently, the proposed dual path control strategy is expected to improve transient response and accelerate recovery from reference speed variations and load disturbances without introducing significant computational complexity. In this study, the difference between reference and actual motor speeds is defined as the speed error, as shown in (1).

$$e(t) = \omega_{ref} - \omega \tag{1}$$

The speed error is processed by the PI controller to generate the inverter reference frequency. The resulting frequency is employed in two parallel processes. First, it is integrated to produce the inverter electrical angle for generating the three-phase sinusoidal reference signals. Second, it is normalized with respect to the motor base frequency to calculate the nominal modulation index (A_{vf}) according to the constant Voltage per Frequency (V/f) principle. This normalization maintains a constant voltage-to-frequency ratio, thereby preserving the air gap magnetic flux over the operating speed range of the induction motor [3], [4].

$$A_{vf} = \frac{|f|}{f_{base}} \tag{2}$$

To enhance the transient response without modifying the fundamental V/f control mechanism, this study introduces a Modulation Index Compensation (MIC) path based on a Proportional Derivative (PD) controller. The PD controller generates a compensation signal that is added to the nominal modulation index to obtain the final modulation index (A_{fin}). Since the modulation index determines the amplitude of the inverter reference voltage in SPWM-based inverters, the proposed compensation enables adaptive voltage regulation during transient operating conditions while preserving the original frequency control strategy [13], [16]. The resulting A_{fin} is subsequently used to generate three sinusoidal reference signals with a 120° phase displacement, as defined in (3)–(5).

$$V_a = A_{fin} sin(\theta) \tag{3}$$

$$V_b = A_{fin} sin(\theta - 120) \tag{4}$$

$$V_c = A_{fin} sin(\theta + 120) \tag{5}$$

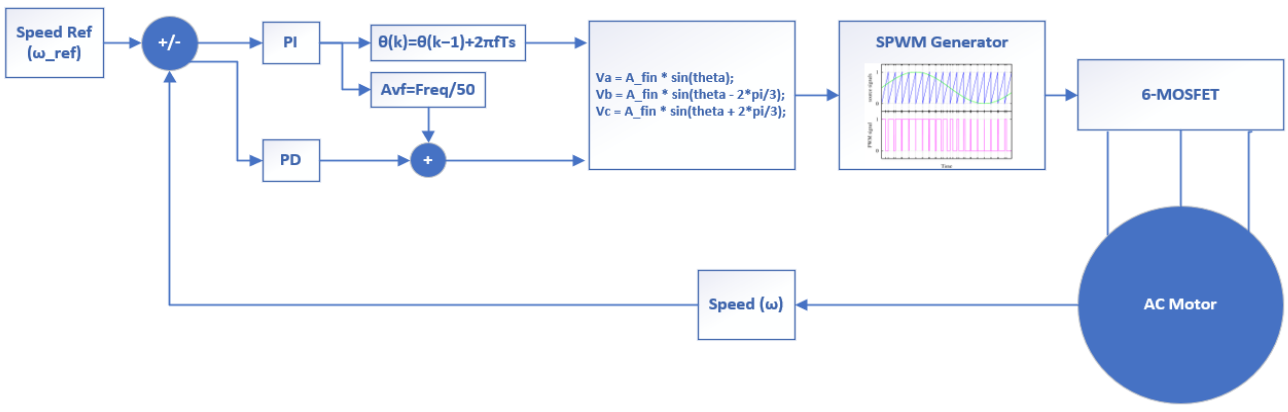


Fig. 1. Block Diagram of Induction Motor Speed Control System Using PI and Modulation Index Compensation.

Vol. 08 No. 2, October-2026, Pages 111-118 DOI: https://dx.doi.org/10.20961/jeeict.8.2.128548
Copyright © 2026 Universitas Sebelas Maret

The three sinusoidal reference signals are then compared with a high-frequency triangular carrier signal in the SPWM generator to produce six gate pulse signals. These PWM signals drive the six switching devices of the three-phase voltage source inverter, thereby generating three-phase AC voltages with the required amplitude and frequency to operate the induction motor [4], [12]. The motor speed is continuously measured and fed back to the controller, forming a closed-loop control system that continuously regulates the motor speed according to the reference command [12], [18].

The primary contribution of this study is the development of a Modulation Index Compensation (MIC) mechanism for a PI-based V/f control system without modifying its fundamental control architecture. In the conventional V/f approach, the PI controller is responsible only for generating the inverter reference frequency, while the output voltage amplitude is determined according to the constant V/f relationship, resulting in the nominal modulation index (A_{vf}). This control strategy is widely adopted because of its simple structure and ease of implementation in inverter-fed induction motor drives [3], [4]. However, because the voltage amplitude follows the predefined V/f relationship, the controller provides limited flexibility for adaptive voltage regulation during transient operating conditions.

In the proposed method, the nominal modulation index is not directly applied as the inverter modulation signal. Instead, it is dynamically adjusted using the output of a Proportional-Derivative (PD) controller, which generates a modulation index compensation signal (A_{com}). To prevent excessive voltage compensation, the (A_{com}) signal is constrained within the range of −0.15 to 0.15 using a saturation limiter. Incorporating the PD controller into the compensation path enables rapid adjustment of the inverter voltage amplitude without affecting the frequency regulation mechanism performed by the PI controller. Consequently, the final modulation index, (A_{fin}), used for SPWM generation is obtained by combining the nominal modulation index with the limited compensation signal, as expressed in (6).

$$A_{fin} = A_{vf} + A_{com} \tag{6}$$

B. PI Control Design

Based on the speed error defined in (1), the PI controller generates the inverter reference frequency, as expressed in (7). This reference frequency serves as the primary control variable for regulating the induction motor speed under the constant V/f control strategy [4].

$$f_{PI} = K_p e(t) + K_i \int e(t)\, dt \tag{7}$$

In this study, the PI controller uses proportional and integral gains of Kp = 0.3 and Ki = 0.5, respectively. These parameters were selected based on the transient response evaluation presented in Section III. The same PI gains are maintained in both the conventional PI-based V/f controller and the proposed PI MIC controller. Therefore, the frequency regulation dynamics remain unchanged in the proposed configuration, while the additional PD-based compensation path provides dynamic adjustment of the inverter modulation index.

The reference frequency generated by the PI controller, f_{PI} is not directly applied to the inverter. Instead, a first-order low-pass filter refere to (8) is employed to smooth variations in the frequency command before it is supplied to the inverter.

$$f = \alpha . f_{PI} + (1 - \alpha) f \tag{8}$$

After filtering, the reference frequency is constrained by a frequency limiter within the range of −50 to +50 Hz to support both forward and reverse motor operation. This bidirectional frequency limitation is consistent with the scalar control implementation [3] . The constrained frequency is subsequently used to calculate the nominal modulation index according to (2), while maintaining the constant Voltage per Frequency (V/f) ratio to preserve the motor air-gap flux during speed regulation [4], [6].

C. Modulation Index Compensation

The nominal modulation index in conventional V/f control is determined solely by the voltage-to-frequency relationship. Consequently, this approach does not provide an additional mechanism to compensate for voltage amplitude variations during transient operating conditions. During acceleration and sudden load variations, the inverter voltage amplitude follows the reference frequency linearly, which may limit the dynamic response of the drive system [4].

To address this limitation, this study proposes a Modulation Index Compensation (MIC) mechanism operating in parallel with the PI controller, as expressed in (9). The PI controller maintains its primary function of regulating the inverter reference frequency, while the additional compensation path dynamically modifies the modulation index to adjust the inverter output voltage amplitude. Previous studies have investigated modulation index compensation to improve voltage regulation and the operating performance of inverter-fed motor drives [19]. Building on this approach, the proposed method incorporates a Proportional Derivative (PD) controller that generates the modulation index compensation signal based on the speed error and its rate of change. This parallel control structure enables dynamic voltage amplitude adjustment during transient conditions without modifying the PI controller gains used for frequency regulation.

$$A_{com} = K_1 e(t) + K_2 \frac{de(t)}{dt} \tag{9}$$

Where A_{com} denotes the modulation index compensation signal, K_1 and K_2 represent the proportional and derivative gains, respectively, and e(t) is the speed error defined in (1). As indicated by (8), the compensation signal is formed by combining the proportional and derivative actions, enabling a rapid response to variations in the speed error.

The proportional component provides an immediate correction proportional to the magnitude of the speed error, whereas the derivative component responds to the rate of change of the error, enabling the controller to anticipate rapid speed variations. Consequently, the combined PD action generates a modulation index compensation signal that dynamically adjusts the inverter voltage amplitude during transient operating conditions. This adaptive voltage regulation enhances the transient performance of the induction motor drive without altering the fundamental frequency regulation mechanism of the conventional V/f control strategy [2], [6].

Copyright © 2026 Universitas Sebelas Maret

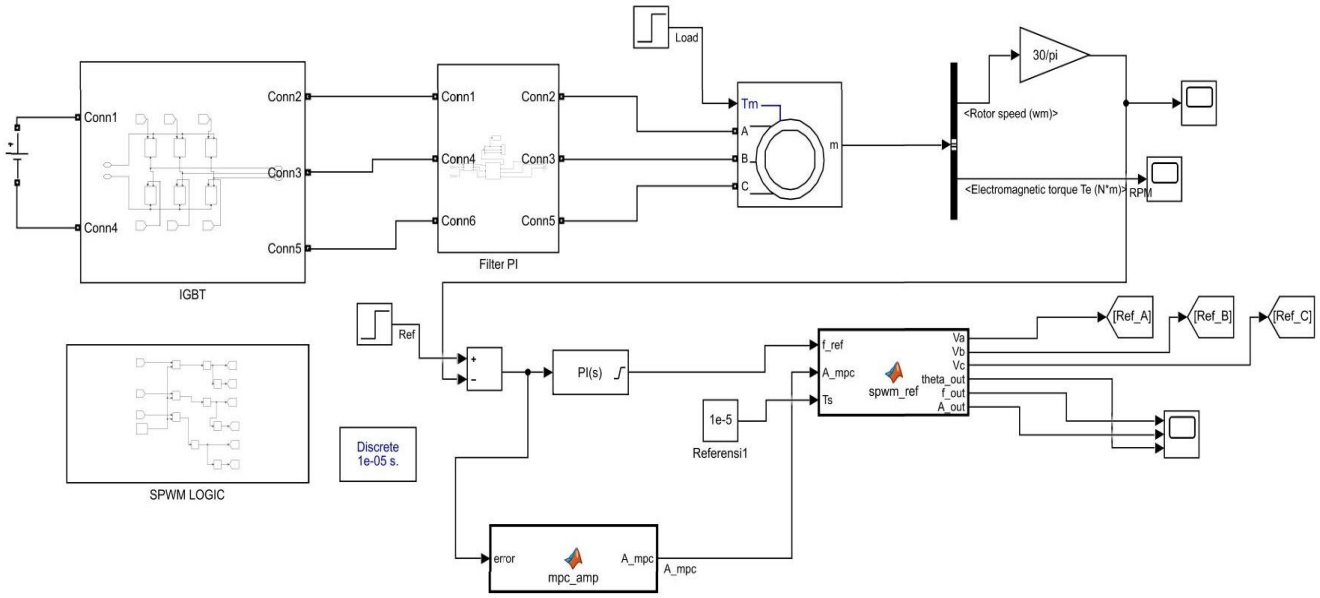


Fig. 2. MATLAB/Simulink model of the proposed induction motor drive system.

The modulation index compensation signal is subsequently added to the nominal modulation index to obtain the final modulation index (A_{fin}), as expressed in (5). The resulting A_{fin} is then constrained using a saturation limiter to ensure that the inverter operates within the linear modulation region ($0.1 \leq A_{fin} \leq 1$). Limiting the modulation index to the linear operating region is a widely adopted approach for maintaining the quality of the inverter output voltage while preventing overmodulation, which may otherwise introduce waveform distortion and increase harmonic components [18].

A lower limit of 0.1 is imposed to provide a low-speed voltage boost, ensuring that the induction motor can generate sufficient starting torque at low operating frequencies. Meanwhile, an upper limit of 1.0 is applied to prevent overmodulation, which may increase harmonic distortion in the inverter output voltage. By enforcing these constraints, the proposed control scheme enables independent regulation of the inverter frequency and voltage amplitude, thereby improving the transient response while preserving the simplicity of the conventional V/f control algorithm

D. SPWM Generation and Three-Phase Inverter

The final modulation index A_{fin} , obtained from the proposed Modulation Index Compensation (MIC), determines the amplitude of the sinusoidal reference signals used for Sinusoidal Pulse Width Modulation (SPWM). In addition to the reference amplitude, SPWM generation requires the inverter electrical angle, which is obtained by integrating the filtered reference frequency generated by the PI controller. The signed reference frequency is maintained during this process to support both forward and reverse motor operation. Consequently, the integration process generates the electrical angle required to produce three balanced sinusoidal reference signals with a phase displacement of 120°. The discrete-time calculation of the inverter electrical angle is expressed in (10) [4], [12].

$$\theta(k) = \theta(k-1) + 2\pi f\, T_s \qquad (10)$$

where θ(k) is the inverter electrical angle at the k-th sampling instant, f is the filtered reference frequency, and T_s is the sampling period, which is set to $1x10^{-5}$. The calculated electrical angle is subsequently substituted into (3)–(5) to generate the three sinusoidal reference signals with a phase displacement of 120 degrees.

E. Simulation Configuration

The proposed Modulation Index Compensation (MIC) method was evaluated through MATLAB/Simulink simulations. The simulation model consists of a DC voltage source, a three-phase voltage source inverter controlled by Sinusoidal Pulse Width Modulation (SPWM), a squirrel cage induction motor, and a closed-loop control system. The control system integrates a Proportional Integral (PI) controller for reference frequency regulation and a Proportional Derivative (PD) controller for modulation index compensation. The simulation was implemented in a discrete-time environment to evaluate the dynamic performance of the proposed control strategy under different operating conditions [4], [12].

The induction motor was modeled using the Asynchronous Machine SI Units block in MATLAB/Simulink. The motor has a rated power of 3.73 kW, a rated voltage of 460 V, and a rated frequency of 60 Hz. The complete MATLAB/Simulink model of the proposed induction motor drive system is illustrated in Fig. 2.

III. RESULT AND DISCUSSION

A. Controller Parameter Optimization Abbreviations and Acronyms

The PI controller parameters were determined by evaluating several combinations of proportional Kp and integral Ki gains. The controller performance was assessed based on rise time, settling time, overshoot, and steady-state error (SSE). The comparison results are summarized in Table I.

Copyright © 2026 Universitas Sebelas Maret

As shown in Table I, the tested PI gain combinations produce different transient responses. All configurations exhibit an identical rise time of approximately 0.299 s. However, the combination of Kp=0.3 and Ki=0.5 achieves the shortest settling time of 0.509 s, with an overshoot of 2.0621% and an SSE of 0.5695 rpm. In contrast, increasing the integral gain to (Ki=2) results in a substantially higher overshoot of 30.364% and a maximum speed of 1303.6 rpm. Based on these results, the PI gain combination of Kp=0.3 and Ki=0.5 was selected for subsequent simulations because it provides the shortest settling time with relatively low overshoot and acceptable steady-state accuracy.

TABLE I. PERFORMANCE COMPARISON OF PI CONTROLLER TUNING

Response	Kp=0.3 Ki=0.3	Kp=0.3 Ki=0.5	Kp=0.4 Ki=0.5	Kp=0.8 Ki=0.5	Kp=0.3 Ki=0.7	Kp=0.3 Ki=2
Tr (s)	0.2990	0.2990	0.2990	0.299	0.299	0.2990
Ts (s)	3.2099	0.5090	0.6408	2.7363	1.1955	1.9236
OS(%)	0	2.0621	4.5864	8.3901	5.9717	30.364
SSE	12.739	0.5695	2.641	7.1579	1.9169	0.0108
Tp (s)	4.9706	0.4373	0.4368	0.4373	0.4448	0.4422
Max (rpm)	987.94	1020.6	1045.9	1083.9	1059.7	1303.6

As shown in Table I, different PI gain combinations produce different transient responses. All configurations exhibit an identical rise time(Tr) of approximately 0.299 s. However, the combination of Kp=0.3 and Ki=0.5 achieves the shortest settling time(Ts) of 0.509 s, with a low overshoot of 2.06% and a steady-state error (SSE) of 0.5695 rpm. In comparison, increasing the integral gain to Ki=2 significantly increases the overshoot (OS) to 30.36% and the peak speed to 1303.6 rpm. Therefore, the PI gain combination of Kp=0.3 and Ki=0.5 was selected for subsequent simulations because it provides a faster settling response with relatively low overshoot and acceptable steady-state accuracy.

B. PD-Based Modulation Index Compensation Parameter Optimization

To determine the appropriate compensation parameters, several combinations of the proportional gain (K1) and derivative gain (K2) were evaluated. The transient performance of each parameter set was assessed using the rise time, settling time, overshoot, and steady-state error (SSE). The results are summarized in Table II, while the corresponding modulation index and speed responses are presented in Fig. 3 and 4, respectively.

TABLE II. PERFORMANCE COMPARISON OF PD COMPENSATION PARAMETERS.

PD-MIC Configuration	Tr (s)	Ts (s)	OS (%)	Tp (s)	Max (rpm)	SSE (rpm)
K1 = 0.0001, K2 = 0.002	0.29916	0.50819	2.0106	0.4372	1020.1	0.4507
K1 = 0.001, K2 = 0.00002	0.29916	0.46219	1.9275	0.3892	1019.3	0.4069
K1 = 0.001, K2 = 0.002	0.29916	0.46219	1.9275	0.3892	1019.3	0.4032
K1 = 0.001, K2 = 0.2	0.29916	0.46238	1.9267	0.3893	1019.3	0.4065
K1 = 0.01 K2 = 0.002	0.29916	0.41965	1.4497	0.3849	1014.5	0.4103

Several combinations of proportional gain K1 and derivative gain K2 were evaluated to determine the appropriate PD-MIC parameters. The performance was assessed based on rise time, settling time, overshoot, peak time, maximum speed, and steady-state error (SSE), as summarized in Table II.

As shown in Table II, the configuration with K_1=0.01 and K2=0.002 achieves the shortest settling time of 0.41965 s and the lowest overshoot of 1.4497%. Although its SSE of 0.4103 rpm is slightly higher than the minimum value of 0.4032 rpm, the difference is relatively small. Therefore, this configuration was selected for subsequent performance evaluation because it provides the best combination of settling time and overshoot among the tested configurations.

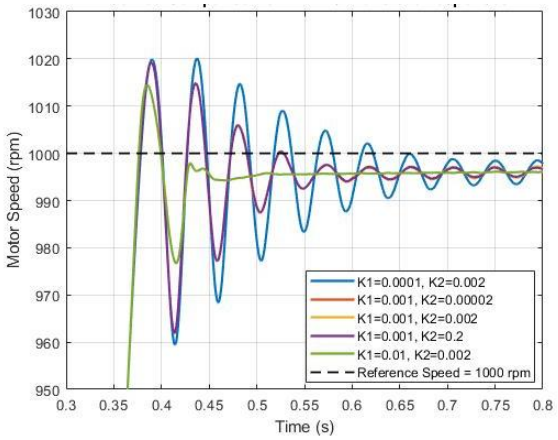


Fig. 3. Speed Response Under Different PD Parameters

Fig. 3 further illustrates the differences in oscillatory behavior among the five configurations. The response with K1 = 0.0001 and K2 = 0.002 exhibits relatively large and prolonged speed oscillations. Increasing K1 to 0.001 reduces the oscillation duration, while the configuration with K1 = 0.01 and K2 = 0.002 provides a faster decay of the transient oscillations. Although the latter configuration produces a slightly higher steady-state error of 0.4103 rpm than the minimum value of 0.4032 rpm obtained with K1 = 0.001 and K2 = 0.002, the difference is only 0.0071 rpm. Considering the improvements in settling time and overshoot, K1 = 0.01 and K2 = 0.002 are selected for the subsequent performance evaluation of the proposed PI-MIC system.

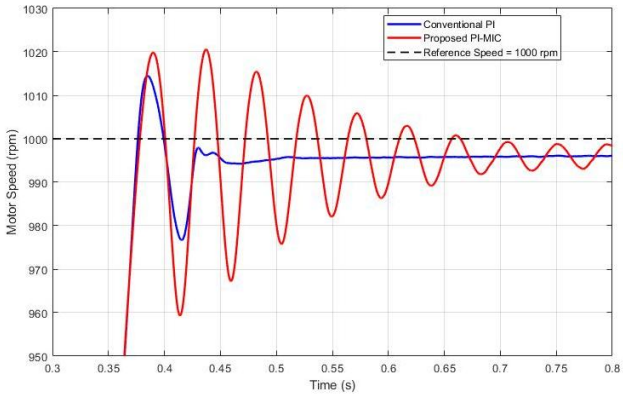


Fig. 4. Comparison of Transient Response

Fig. 4 compares the transient speed responses of the conventional PI and proposed PI-MIC controllers. The conventional PI controller uses Kp=0.3 and Ki=0.5, while the PI-MIC controller employs K1=0.01 and K2=0.002. Both controllers exhibit nearly identical rise times of approximately 0.299 s. However, PI-MIC achieves a shorter settling time of 0.41965 s compared with 0.5090 s for

Copyright © 2026 Universitas Sebelas Maret

conventional PI, representing a reduction of 17.55%. The overshoot also decreases from 2.0621% to 1.4497%. Furthermore, the peak time decreases from 0.4373 s to 0.3849 s, while the maximum speed decreases from 1020.6 rpm to 1014.5 rpm. The SSE also decreases from 0.5695 rpm to 0.4103 rpm. These results indicate that the proposed PI MIC improves the measured transient response and steady-state accuracy under the evaluated simulation conditions.

Table I summarizes the tuning results of the conventional PI controller, while Table II presents the optimization results of the PD-based modulation index compensation parameters. The PI gains of Kp = 0.3 and Ki = 0.5 were maintained throughout the PD-MIC parameter evaluation. Among the tested PD configurations, K1 = 0.01 and K2 = 0.002 provide the shortest settling time of 0.41965 s and the lowest overshoot of 1.4497%. These results support the selection of this parameter combination for subsequent PI-MIC performance evaluations. However, the tuning results in Tables I and II represent separate parameter optimization processes and should not be interpreted as a direct quantitative comparison between the conventional PI and PI-MIC controllers. A direct performance comparison requires transient response metrics extracted from both configurations under identical simulation conditions.

TABLE III. STEADY-STATE THD COMPARISON BETWEEN PI-MIC AND CONVENTIONAL PI.

Parameter	Conventional PI	Proposed PI-MIC	THD Reduction
Voltage THD (%)	1.61	1.27	21.12%
Current THD (%)	10.44	2.31	77.87%

Table III compares the steady-state harmonic distortion of the conventional PI and proposed PI-MIC controllers. The PI-MIC strategy reduces voltage THD from 1.61% to 1.27% and current THD from 10.44% to 2.31%, corresponding to reductions of 21.12% and 77.87%, respectively. These results indicate that the proposed PI-MIC strategy improves the harmonic characteristics of the inverter output, particularly the motor current.

C. Performance Under Load Disturbance

To evaluate the robustness of the proposed control strategy under varying operating conditions, a load disturbance test was conducted by applying a 5 Nm load torque at t=3 s. The dynamic responses of the conventional PI controller and the proposed Modulation Index Compensation (MIC) were compared under identical simulation conditions. The resulting speed responses are presented in Fig. 5, while the corresponding quantitative performance metrics are summarized in Table IV.

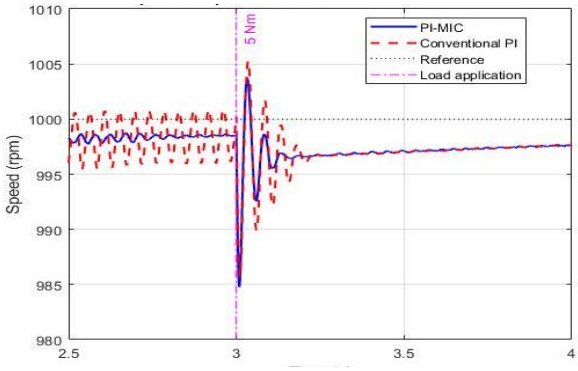


Fig. 5. Speed Response Under an 5 Nm Load Disturbance

TABLE IV. DYNAMIC PERFORMANCE UNDER LOAD DISTURBANCE

Parameter	PI-MIC	Conventional PI
Initial Speed (rpm)	998.47	998.32
Minimum Speed (rpm)	984.76	985.65
Speed Dip (rpm)	13.703	12.674
Speed Dip (%)	1.3724	1.2695
Peak Recovery Speed (rpm)	1003.7	1005.3
Recovery Time (s)	0	0
Steady-State Error (rpm)	1.0345	1.0338
Recovery Oscillation (rpm)	0.049881	0.049114
THD-V (%)	2.02	2.05
THD-I (%)	2.45	2.39

Fig. 5 illustrates the speed responses of the proposed PI-MIC and conventional PI controllers under a 5 Nm load disturbance applied at 3 s. Both controllers experience a speed reduction followed by recovery toward the reference speed. The PI-MIC controller exhibits a slightly larger speed dip of 13.703 rpm compared with 12.674 rpm for the conventional PI controller. However, PI-MIC produces a lower recovery peak of 1003.7 rpm, compared with 1005.3 rpm for the conventional PI. Both controllers also exhibit nearly identical steady-state errors of 1.0345 rpm and 1.0338 rpm, respectively. Regarding harmonic performance, PI-MIC achieves slightly lower voltage THD (2.02% versus 2.05%), while its current THD is marginally higher (2.45% versus 2.39%). These results indicate that PI-MIC provides a comparable disturbance response, with a lower recovery peak, but does not consistently outperform conventional PI across all evaluated parameters.

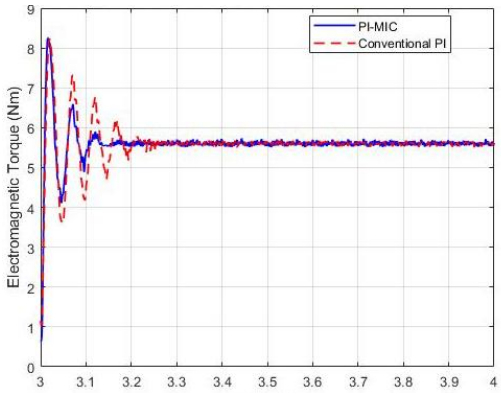


Fig. 6. Electromagnetic Torque Comparison – Load Disturbance

TABLE V. ELECTROMAGNETIC TORQUE PERFORMANCE COMPARISON UNDER 5 NM LOAD DISTURBANCE

Parameter	PI-MIC	Conventional PI
Initial Torque (Nm)	0.60137	0.63402
Maximum Torque (Nm)	8.2599	8.2343
Minimum After Peak (Nm)	4.1053	3.6269
Torque Peak Deviation (Nm)	7.6586	7.6003
Torque Peak Deviation (%)	1273.5	1198.7
Peak Time (s)	0.015904	0.019876
Minimum Torque Time (s)	0.045680	0.049801
Settling Time (s)	0.12086	0.19491
Steady-State Torque (Nm)	5.6029	5.6030
Steady-State Torque Deviation (Nm)	5.0015	4.9689
Torque Ripple Std (Nm)	0.041069	0.033339
Peak-to-Peak Ripple (Nm)	0.20997	0.15989

Fig. 6 illustrates the electromagnetic torque responses of the proposed PI-MIC and conventional PI controllers under a 5 Nm load disturbance applied at 3 s. As summarized in Table V, both controllers produce similar maximum torque values of approximately 8.2 Nm. However, PI-MIC achieves a higher minimum torque after the first peak 4.1053 Nm than

Vol. 08 No. 2, October-2026, Pages 111-118 DOI: https://dx.doi.org/10.20961/jeeict.8.2.128548
Copyright © 2026 Universitas Sebelas Maret

conventional PI 3.6269 Nm, indicating a smaller torque reduction during the initial transient response. Furthermore, PI MIC reduces the settling time from 0.19491 s to 0.12086 s, corresponding to a 38.0% improvement. This result is consistent with Fig. 6, where the PI MIC response exhibits faster oscillation attenuation following the disturbance. Nevertheless, conventional PI produces lower steady-state torque ripple, with a standard deviation of 0.03334 Nm compared with 0.04107 Nm for PI MIC. These findings indicate that the proposed PI MIC strategy improves transient torque recovery, although its steady-state torque ripple remains slightly higher than that of conventional PI control.

D. Impact of Inverter Dead Time on PI MIC Control Performance

In practical voltage source inverters, dead-time is introduced between the switching signals of complementary power semiconductor devices to prevent short-circuit conditions in each inverter leg. However, this switching delay can cause voltage distortion and alter the inverter output characteristics, potentially affecting the performance of induction motor drives. Therefore, evaluating the proposed PI MIC strategy under different dead time conditions is necessary to assess its performance under non-ideal inverter switching conditions. This investigation examines the influence of inverter dead time variations on the speed response, electromagnetic torque, and harmonic characteristics of the induction motor drive. The results provide insight into the sensitivity of the proposed PI MIC controller to inverter dead-time effects.

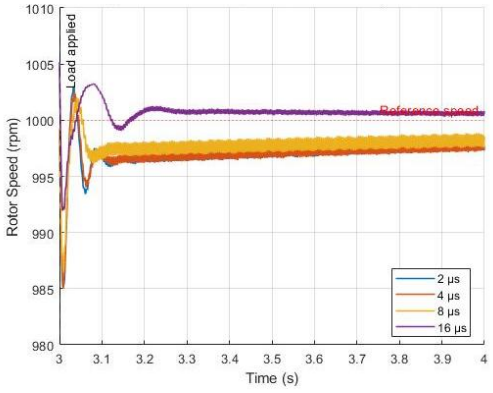


Fig. 7. Speed Transient Response after Load Application

TABLE VI. SPEED RESPONSE PERFORMANCE UNDER DIFFERENT DEAD-TIME CONDITIONS AFTER LOAD APPLICATION

Performance Parameter	2 µs	4 µs	8 µs	16 µs
Pre-load speed (rpm)	998.36	998.63	999.85	1005.10
Minimum speed (rpm)	985.07	984.99	986.52	991.95
Speed dip (rpm)	13.291	13.643	13.326	13.112
Speed dip (%)	1.3313	1.3662	1.3328	1.3046
Recovery peak (rpm)	1003.0	1002.6	1002.0	1003.3
Recovery peak time (s)	0.03343	0.03501	0.04066	0.08103
Recovery overshoot (%)	0.30175	0.25919	0.20189	0.32602
Loaded steady-state error (rpm)	1.6343	1.5586	1.1734	0.38586

Fig. 7 shows the rotor speed response following load application at t = 3 s under different inverter dead-time conditions. All configurations exhibit a speed dip followed by recovery toward the reference speed. As presented in Table VI, the speed dip ranges from 13.112 to 13.643 rpm, indicating relatively consistent speed regulation across the tested conditions. The 16 µs setting produces the smallest speed dip of 13.112 rpm, but also results in the longest recovery peak time of 0.08103 s. Meanwhile, the loaded steady-state error decreases from 1.6343 rpm at 2 µs to 0.38586 rpm at 16 µs. These results indicate that inverter dead time influences the transient recovery characteristics of the PI-MIC controlled induction motor..

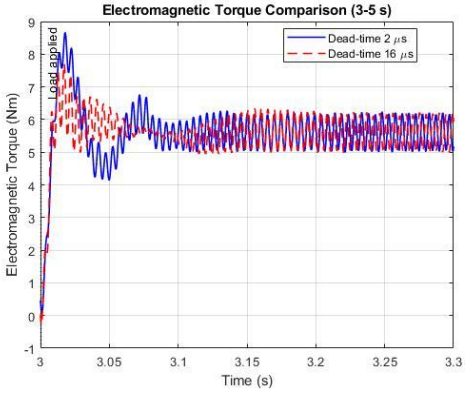


Fig. 8. Electromagnetic Torque Comparison after Load Application

TABLE VII. TRANSIENT TORQUE PERFORMANCE UNDER DIFFERENT DEAD-TIME CONDITIONS AFTER LOAD APPLICATION

Performance Parameter	2 µs	4 µs	8 µs	16 µs
Initial Torque (Nm)	0.60122	0.60489	0.60283	0.60308
Maximum Torque (Nm)	8.6675	8.7832	9.3212	7.6981
Minimum After Peak (Nm)	4.1397	3.7841	3.7397	4.9031
Peak Deviation (Nm)	8.0663	8.1783	8.7183	7.0950
Peak Time (s)	0.01790	0.01937	0.01550	0.01721
Minimum Time (s)	0.04985	0.05133	0.05679	0.12463
Settling Time (s)	0.07331	0.07565	0.07898	0.06177

Fig. 8 shows the electromagnetic torque response following load application at t = 3 s under different inverter dead-time conditions. The torque increases rapidly before exhibiting transient oscillations and approaching the loaded steady-state condition. As reported in Table VII, the maximum torque ranges from 7.6981 Nm at 16 µs to 9.3212 Nm at 8 µs. The 16 µs setting also produces the highest minimum torque after the peak of 4.9031 Nm and the shortest settling time of 0.06177 s. These results indicate that inverter dead time affects the transient torque response, particularly the peak torque and settling time of the PI-MIC controlled induction motor.

TABLE VIII. VOLTAGE AND CURRENT THD UNDER DIFFERENT INVERTER DEAD-TIME CONDITIONS AFTER LOAD APPLICATION

Dead-time (µs)	Voltage THD (%)	Current THD (%)
2	3.95	7.75
4	6.22	14.36
8	10.49	22.14
16	14.38	16.58

Table VIII presents the voltage and current THD under different inverter dead-time conditions. The voltage THD increases from 3.95% at 2 µs to 14.38% at 16 µs. Meanwhile, the current THD reaches its highest value of 22.14% at 8 µs before decreasing to 16.58% at 16 µs. The lowest voltage and current THD values occur at 2 µs, indicating the best harmonic performance among the tested conditions. These results show that inverter dead time affects voltage and current distortion differently.

Vol. 08 No. 2, October-2026, Pages 111-118 DOI: https://dx.doi.org/10.20961/jeeict.8.2.128548
Copyright © 2026 Universitas Sebelas Maret

IV. CONCLUSION

This study proposed a PD-based Modulation Index Compensation (MIC) strategy integrated into a PI-based V/f control system for a three-phase induction motor. The proposed method uses a PD controller to adjust the inverter modulation index while maintaining the PI controller for frequency regulation.

Simulation results show that the selected PI-MIC configuration improves the startup transient response compared with conventional PI control. The settling time decreases from 0.5090 s to 0.41965 s, while the overshoot decreases from 2.0621% to 1.4497%. The steady-state error also decreases from 0.5695 rpm to 0.4103 rpm. Under a 5 Nm load disturbance, PI-MIC produces a slightly larger speed dip than conventional PI, but achieves a lower recovery peak and comparable steady-state error. The torque response also shows a shorter settling time of 0.12086 s compared with 0.19491 s for conventional PI, although the torque ripple is slightly higher.

The dead-time evaluation further demonstrates that inverter switching delay affects the speed, torque, and harmonic characteristics of the drive system. A dead time of 2 µs provides the lowest voltage and current THD, while larger dead-time values produce different transient responses. These findings indicate that the proposed PI-MIC strategy improves selected transient performance indicators, but its effectiveness depends on the operating and inverter switching conditions. Future work will focus on experimental validation using a three-phase inverter prototype.

ACKNOWLEDGMENT

The author(s) disclosed receipt of the following financial support for the research, authorship, and/or publication of this article: This work was supported by the Politeknik Negeri Jakarta [grant numbers 348/DST/PL3.14/B/PT.00.03/2026].

REFERENCES

[1] D. Zellouma, H. Benbouhenni, N. Bizon, and Y. Bekakra, "A New Field-Oriented Control for Induction Motor Drive Using a Synergetic-Super Twisting Algorithm," in *2023 15th International Conference on Electronics, Computers and Artificial Intelligence (ECAI)*, Jun. 2023, pp. 1–6. doi: 10.1109/ECAI58194.2023.10193989.

[2] Y. Bendaha, K. Boumediene, and B. Daaou, "A Comparative Study of Conventional and Advanced PI Controllers for Induction Motor Speed Regulation under Parameter Variations," *Acta Mech. Autom.*, vol. 20, pp. 227–234, 2026, doi: 10.65731/ama/2026-0023.

[3] O. Al-khamis, "Study of performance the 3-phase induction motor that drives by using scalar and vector control with variable speed loading," *Indones. J. Electr. Eng. Electron.*, vol. 41, pp. 894–911, 2026, doi: 10.11591/ijeecs.v41.i3.pp894-911.

[4] S. K. Purella, A. P. Raju, and K. U. Devi, "Simulation and development of inverter fed three phase induction motor using V/f control strategy," Int. J. Eng. Res. Sci. Technol., vol. 22, no. 2, pp. 287–297, 2026, doi: 10.62643/ijerst.2026.v22.n2(3).3610.

[5] K. Sun and W. Niu, "SPWM Inverter Control for Wireless Constant Current and Voltage Charging," *World Electr. Veh. J.*, vol. 14, no. 4, 2023, doi: 10.3390/wevj14040111.

[6] I. Irianto, F. D. Murdianto, E. Sunarno, and D. D. Proboningtyas, "Comparison Method of PI, PID and Fuzzy Logic Controller to Maintain Speed Stability in Single Phase Induction Motors," *INTEK J. Penelit.*, vol. 8, no. 1, pp. 7–16, 2021, doi: 10.31963/intek.v8i1.2687.

[7] B. S. Winslet, K. Preethi, K. S. Krishna, and J. S. V. Prasad, "Performance of Induction Motor using V/F Control Technique," in *2022 IEEE 2nd Mysore Sub Section International Conference (MysuruCon)*, Oct. 2022, pp. 1–6. doi: 10.1109/MysuruCon55714.2022.9972542.

[8] M. Alathamneh, H. Ghanayem, R. M. Nelms, and I. M. Allafi, "Open-Circuit Fault Mitigation for Inverter-Driven Induction Motor Based on Closed-Loop Volt-per-Hertz," *Energies*, vol. 18, no. 7, 2025, doi: 10.3390/en18071596.

[9] R. Yadav, M. Kar, and A. Singh, "Speed control of a three-phase IM with closed-loop control scheme," in Advances in Power Systems and Energy Management, Singapore: Springer, 2022, pp. 43–55, doi: 10.1007/978-981-16-9239-0_4.

[10] S. Zhang *et al.*, "An Improved SPWM Strategy for Effectively Reducing Total Harmonic Distortion," *Electronics*, vol. 13, no. 16, 2024, doi: 10.3390/electronics13163326.

[11] R. Sreedhar, S. K. B. Pradeepkumar Ch, K. Karunanithi, S. Ramesh, B. Pasupulati, and A. Dhinakaran, "A Novel Hybrid SPWM and SHEPWM-based Three-Phase Inverter for Induction Motor Control," *2024 Int. Conf. Comput. Intell. Green Sustain. Technol. ICCIGST 2024 - Proc.*, pp. 1–6, 2024, doi: 10.1109/ICCIGST60741.2024.10717548.

[12] R. Borthakur and A. B. Kandali, "Design and simulation of a three-phase induction motor for speed control using constant V/f technique with sinusoidal PWM-based inverter," *Int. J. Innov. Technol. Explor. Eng.*, vol. 14, no. 9, pp. 12–20, 2025, doi: 10.35940/ijitee.I1120.14090825.

[13] D. Sendima and P. M. Makolo, "Investigating the Harmonic Content of a PWM Inverter with Varying Modulation Index," *Tanzania J. Eng. Technol.*, vol. 43, no. 3, pp. 34–48, 2026, doi: 10.65085/2619-8789.1001.

[14] L. Xing, Q. Wei, Y. Li, and Y.-F. Liu, "Phase-Shifting SPWM-Based Modulation for Single-Source Five-Level Current Source Inverter," *IEEE Trans. Power Electron.*, vol. 40, no. 8, pp. 10343–10348, Aug. 2025, doi: 10.1109/TPEL.2025.3553027.

[15] Suroso, H. Prasetijo, H. Susilawati, E. Murdyantoro, and A. Mubyarto, "Modified multicarrier sinusoidal pulse-width modulation for three-phase open-load five-level inverter," *Bull. Electr. Eng. Informatics*, vol. 13, no. 6, pp. 3910–3918, 2024, doi: 10.11591/eei.v13i6.7899.

[16] A. Sharma and A. Singhal, "Designing of Three Level 3 Phase Inverter Using Improved SPWM Modulation for different Loads," *Turkish J. Comput. Math. Educ.*, vol. 12, no. 3, pp. 4513–4520, 2021, [Online]. Available: https://engineering-journals.org/journals/turcomat/turcomat-volume-12-issue-3/designing-of-three-level-3-phase-inverter-using-improved-spwm-modulation-for-different-loads/

[17] Y. Ji and Y. Xu, *Analysis of Three-Phase Inverter SPWM Modulation Strategy*, vol. 1, no. 1. Association for Computing Machinery, 2025. doi: 10.1145/3702191.3708490.

[18] E. Nandhini and A. Sivaprakasam, "A New Closed Loop Constant v/f Control of Induction Motor with Torque Control Based on DPWM," *Int. J. Electr. Electron. Res.*, vol. 11, no. 2, pp. 523–528, 2023, doi: 10.37391/ijeer.110239.

[19] L. Shen *et al.*, "Beat-less algorithm based on dual-frequency compensation in railway traction applications," *IET Power Electron.*, vol. 14, no. 11, pp. 1985–1994, 2021, doi: 10.1049/pel2.12164.

Copyright © 2026 Universitas Sebelas Maret